2021

Exploring the Role of the PKHD1L1 Gene in Epithelial Cancer Cells

Bella Kohrs
Denison University

Exploring the Role of the PKHD1L1 Gene in Epithelial Cancer Cells

Bella Kohrs
Faculty Advisor: Dr. Lina Yoo
Year of Study: 2020-2021
Department of Biology

Exploring the Role of the PKHD1L1 Gene in Epithelial Cancer Cells

Bella Kohrs

Advisor: Dr. Lina Yoo

Cancer is the second leading cause of death in the United States and there is still no cure. This disease is caused, at least in part, by the accumulation of genetic mutations. Polycystic kidney and hepatic disease 1-like 1 (PKHD1L1) is one such gene that is highly mutated and downregulated in epithelial cancers and is thus thought to function as a tumor suppressing gene. However, its function and protein are still poorly understood. The purpose of this research is to further explore the role of PKHD1L1 as a potential tumor suppressor by localizing its protein within the cell. In order to achieve this localization, we engineered both pFETCh and pspCas9 vectors in an attempt to insert the well characterized FLAG-tag near the stop codon of the PKHD1L1 gene. Once the plasmids were successfully assembled, they were co-transfected into 293 kidney cells. Transfected kidney cells were selected with G418 antibiotic, fixed, and stained with 9A3 mouse Flag antibody and secondary anti-mouse fluorescent antibody. Subsequent visualization of the FLAG-tag alongside nuclear staining indicated that the PKHD1L1 protein appears to be a cytoplasmic. Further investigation into the precise location of the protein within the cytoplasm is necessary, but this novel localization could provide insight into the potential function of PKHD1L1 as a tumor suppressing gene.

Introduction

Cancer is a disease which has been extensively researched. However, despite the vast amount of effort that has been put into learning about and understanding the pathology, there is still no cure. Second only to heart disease, cancer is one of the leading causes of death in the United States (Center for Disease Control and Prevention). As of 2017 when the last incidence data are available, the CDC United States cancer statistics show that female breast cancer is the most prevalent type of cancer to be presented in new cancer cases. Furthermore, lung/bronchus and female breast cancer have the highest death rates out of all cancer types. Interestingly, both lung/bronchus and breast cancer are carcinomas, meaning that they originate from the tissue that covers the body and lines its internal cavities, called the epithelium. These epithelial cancers, which include types of lung/bronchus, breast, colon, bladder, and skin cancers make up 80-90% of all cancer cases (Center for Disease Control and Prevention & National Cancer Institute).

The "Two-Hit" Model

Unfortunately, there is no one cause of cancer. Research points to a variety of risk factors that may play a role in the development of neoplasia ranging from dietary influences to genetic predispositions (Knudson, 1993; Giovannucci & Willett, 1994; Knudson, 1996). However, a consistent theme in cancer development is that numerous genetic changes over a period of time appear to underlie abnormal cell growth and division (Kinzler & Vogelstein, 1996). Although these changes can happen anywhere in the genome, a common site of mutation in cancers occurs in what are known as antioncogenes, or tumor suppressor genes. These genes, when intact, are generally negative regulators of cell growth, meaning that when they are mutated, uncontrolled growth, and subsequently cancer, can occur (Knudson, 1993). In regard to genetic predisposition,

it has been observed that dominantly inherited cancers can often be attributed to inheriting at least one mutated copy of a tumor suppressor gene. However, the presence of heterozygosity for an antioncogene gene is not sufficient for cancer development, meaning that the mutated gene demonstrates incomplete penetrance. Therefore, inherited germline mutations count as the first "hit" to a tumor suppressor gene (Knudson, 1993).

In order to understand what a singular "hit" to an antioncogene implies, it is important to look at the "two-hit" model of neoplasia development. Within this model, it is posited that in order to develop a tumor, an individual must acquire either two somatic mutations (in non-hereditary cases) or one germline and one somatic mutation (in cases of an inherited predisposition) to the homologous copies of a gene, often a tumor suppressor (Knudson, 1996). However, although in some cases these two hits are sufficient to produce neoplasia, in other cases more genetic alterations are needed. The number of necessary mutations can vary from just a few to many. For example, in colorectal cancers, at least seven genetic alterations are necessary for neoplasia (Kinzler & Vogelstein, 1996). Inheriting even one mutation in this sequence can lead to predisposition, but the more mutations that are necessary to result in neoplasia, the more the impact of the inherited germline predisposition decreases. Thus far, there is no known mutation that, when inherited, would predispose an individual to any/all types of cancer (Knudson, 1996).

Tumor Suppressor Genes– "Gatekeepers" and "Caretakers"

Given that no known mutation results in universal predisposition to all cancer types, it is evident that a cancerous mutation appears to have an element of specificity. This specificity occurs because in epithelial cancers, the tissue in which the gene is mutated is generally the

tissue in which the cancer will arise (Kinzler & Vogelstein, 1997). Therefore, if a tumor suppressor gene is mutated in the breast tissue, neoplasia may develop in the breast. In order to understand the cancer development in these tissues, it is important to approach the topic of tumor suppressor function. As was previously mentioned, tumor suppressors are the genes that are more frequently mutated in cancerous tissues (Knudson, 1993). However, antioncogenes do not have a universal function, but rather generally fall under the category of either "gatekeepers" or "caretakers". In 1996 and 1997 studies by Kinzler and Vogelstein, these two categories of antioncogenes were described in depth. "Gatekeeper" genes have been implicated in general control of cell division, cell growth in response to tissue damage, as well as general cell lifespan/apoptosis, which is how they directly regulate potential tumor growth. One can thus deduce that when gatekeeper genes are mutated, cancer can result due to decreased regulation of cell growth and apoptosis. Interestingly, gatekeepers don't appear to be incredibly abundant, with cell types only containing a few or even just one of these genes. Therefore, if even one of the few gatekeepers present is compromised, such a mutation can allow for overgrowth of the cells and cancer progression (Kinzler & Vogelstein, 1996; Kinzler & Vogelstein, 1997).

As was discussed earlier, gatekeeper genes fit within the "two-hit" model since for a tumor to be able to develop, both maternal and paternal copies of the gene must be knocked down. Individuals with gatekeeper predispositions are at increased risk of developing cancer due to the fact that they have one germline mutation and only need to acquire one additional somatic mutation for the regulation of cell growth to be compromised. More specifically, these individuals' risk of developing cancer is $>10^3$ higher than the average, non-predisposed person. Although it is possible for people without germline mutations to develop cancer through mutation of a gatekeeper gene, it is less likely than for people who are predisposed because there

is a greater chance of acquiring a single somatic mutation rather than two in the same location on each copy of the allele (Kinzler & Vogelstein, 1997).

In contrast to gatekeeper genes, which directly regulate cell growth, Kinzler and Vogelstein discuss how the other category of antioncogenes, called “caretakers”, function more indirectly as they aid in genome stability. The mutation of a caretaker gene does not directly promote tumor growth, but can instead lead to genetic instability, which in turn leads to more frequent mutations in gatekeeper genes and thus neoplasia (Kinzler & Vogelstein, 1997). Individuals who inherit one mutant copy of a caretaker gene have a risk of developing cancer that is 5-50 fold higher than non-predisposed individuals (Kinzler & Vogelstein, 1996). Although high, this risk of developing cancer is significantly lower than the risk for individuals who are predisposed to gatekeeper mutations. This difference is due to the fact that if an individual inherits a gatekeeper mutation, they only need to acquire one more somatic mutation to develop neoplasia. In contrast, if one inherits a caretaker mutation, that individual needs to acquire a minimum of three more somatic mutations to develop neoplasia (the second caretaker mutation as well as both gatekeeper mutations). The difference in the risk of predisposition to gatekeeper and caretaker mutations also means that spontaneous development of cancer originating from a caretaker gene is expected to be infrequent because one would need to develop four somatic mutations, which is statistically less likely to occur. (Kinzler & Vogelstein, 1996). One promising finding, however, is that mutations to caretaker genes provide the opportunity for a therapeutic target because tissues with such mutations appear to be more sensitive to therapeutic agents that cause the type of damage that the mutated caretaker gene product would normally recognize and repair (Kinzler & Vogelstein, 1997).

Tumor Suppressor Genes– BRCA1 and BRCA2

In order to understand the function of these gatekeeper and caretaker tumor suppressor genes in epithelial cancers, it is useful to look at the well-studied examples of the BRCA1 and BRCA2 genes. Although the gene products of BRCA1 and BRCA2 have very little resemblance to each other or to other proteins whose functions are known, they have both been implicated in playing a role in DNA repair, DNA recombination, checkpoint control of the cell cycle, transcription, and preserving chromosome structure. Therefore, mutations to BRCA1 and BRCA2 have also been observed to result in a notable predisposition to breast cancer (Venkitaraman, 2002). As was mentioned above, only one defective copy of either gene is required to be at risk of cancer, although the second allele is often observed to be mutated in tumor cells. Interestingly, both BRCA1 and BRCA2 appear to function as caretakers because when they are deficient, the chromosomes of mutated cells exhibit chromosome abnormalities such as breakages, translocations, deletions, and fusions across non-homologous pairs. Furthermore, as this finding supports, the protein products of these genes have been found to localize to the nucleus (Venkitaraman, 2002).

Within the nucleus, a study by the Sharan research group in 1997 found that BRCA1 appears to interact with proteins that may be involved in the repairs of double stranded DNA breaks, supporting its role as a caretaker gene. Therefore, if BRCA1 is mutated and cannot properly form the necessary interactions with these proteins, they may not be able to appropriately repair double stranded breaks, which would then result in genome instability. This finding also indicates that the proteins that BRCA1 interacts with may also be antioncogenes if they are necessary for DNA repair/genome stability and thus tumor suppression. Furthermore, repairing double stranded breaks also plays a role in controlling cell-cycle progression meaning

that if the BRCA1 gene is mutated and the protein is deficient, the cell-cycle may continue abnormally (Sharan et al., 1997).

Introduction to PKHD1L1

This introduction into epithelial cancers, antioncogenes and the well characterized examples of BRCA1 and BRCA2 provides context for the gene of interest in this study– polycystic kidney and hepatic disease 1-like 1, often called PKHD1L1. As a brief overview, PKHD1L1 is a gene that is hypothesized to aid the body in suppressing tumors and is commonly mutated in cancers such as skin, bladder, breast, and colon cancer (NCI Genomic Data Commons). While little research has been conducted on PKHD1L1, researchers have found that the levels of mRNA in skin, bladder, colon, etc. tumors, where the gene is mutated, are lower than in normal, healthy tissues (Grossman *et al*, 2016). Such findings indicate that irregularities in the gene cause a deficit of mRNA which may in turn lead to a decrease in the production of proteins that are vital to helping the body suppress tumors. Overall, however, PKHD1L1 is still poorly understood.

Previous research on PKHD1L1 has implicated the gene in a variety of possible functions ranging from playing a role in male longevity to functioning as a tumor suppressor (Erdman et al., 2015; Zheng et al., 2019). A 2019 study by Wu et al. found that PKHD1L1 may play a role in hearing in mice. Interestingly, this research group also stated that PKHD1L1 is mostly extracellular although this cannot be certain due to the fact that the protein has not yet been localized in cells. Based on other stereocilia link proteins, the authors hypothesized that PKHD1L1 would be large, i.e., greater than 1500 amino acids and likely closer to 4000, and that the protein may have one, although potentially more than one, transmembrane domain. However,

PKHD1L1 appears to only have a single transmembrane domain near the C-terminus so it would differ from other stereocilia link proteins in this regard (Wu et al., 2019).

Based on their findings, Wu et al. noted that the PKHD1L1 protein appears to be expressed at the tips of the inner ear hair cells of mice, called stereocilia, and may play a role in forming the surface coat of these cells. When PKHD1L1 was knocked out, mice developed hearing loss and appeared not to have a surface coat in the upper region of the stereocilia. Although it appeared as if the stereocilia bundles were able to develop normally, the cell protein coat distribution was affected, leaving the upper cell surface uncoated in PKHD1L1-deficient mice. Antibody labeling indicated increased levels of the PKHD1L1 protein in hair cells and further imaging showed that the gene product was located mostly between stereocilia, which would support the hypothesis that the protein is extracellular (Wu et al., 2019). However, the Novus Bio Cat#NBP2-13765 antibody that was used for labeling has since been discontinued, which may set into question its efficacy and the validity of the results observed in this study.

Aside from potentially contributing to the protein coat of stereocilia, PKHD1L1 is also thought to play a role in autosomal recessive polycystic kidney disease, from which the gene received its name, as well as cellular immunity (Hogan et al., 2003; Lian et al., 2011). PKHD1L1 is a homolog of both PKHDL1 and PKHD1. PKHD1 is a gene that encodes fibrocystin and when mutated, the gene causes autosomal-recessive polycystic kidney disease (ARPKD). PKHDL1 is a homolog of PKHD1 and codes for fibrocystin-L. However, upon investigation, no evidence of PKHDL1 mutations in ARPKD patients were found, indicating that it may not be involved in the disease. Since PKHD1L1 is another homolog of the PKHD1 gene, it is thought that the PKHD1L1 may play a role in ARPKD. Furthermore, PKHD1L1 is thought to potentially participate in cellular immunity since it is a homolog of PKHDL1, which encodes fibrocystin-L–

a protein that participates in cellular immunity (Hogan et al., 2003; Lian et al., 2011). However, neither of these hypotheses have been supported by research to date.

Two separate and more recent studies support the function of PKHD1L1 as a potential tumor suppressor gene (Zheng et al., 2019; Wang et al., 2020). In 2019, the Zheng research group explored the expression patterns of PKHD1L1 in thyroid cancer tissue and found that gene expression was significantly downregulated in cancerous thyroid tissue compared to normal tissue. This downregulation was also significantly associated with various clinicopathological features including lymph node metastasis, distant metastasis, tumor size, clinical stage of cancer, as well as increased proliferation, migration, and invasion capabilities of the cancerous cells. These findings indicate that when active, PKHD1L1 appears to counteract these cellular behaviors and may therefore function as a tumor suppressor (Zheng et al., 2019). The Wang research group further supported this finding in their 2020 analysis of data from the Cancer Genome Atlas (TCGA). In this study, Wang et al. found that PKHD1L1 appears to be associated with the prognosis of lung adenocarcinomas (LUAD). It was discovered that PKHD1L1 had a single nucleotide polymorphism (SNP) mutation site at rs768349010 that was significantly related to its gene expression. The GG version of the SNP resulted in decreased expression of PKHD1L1 compared to the wild-type GA SNP. This study also found that the overall survival of patients was lower for individuals with low expression of PKHD1L1 compared to individuals with higher expression of the gene, indicating once again that PKHD1L1 may be acting as a tumor suppressor (Wang et al., 2020).

Proposed Investigation of PKHD1L1

Given these findings, the purpose of this research project is to further explore the potential tumor suppressing function of PKHD1L1 in epithelial cancer cells. Since very little research has been published about the protein itself, we aim to learn more about the function of PKHD1L1 by localizing its protein in the cell. Improper localization, or lack thereof, can contribute to the development of a variety of diseases, including cancer. Therefore, determining the cellular location of a protein can help to provide context for its function (Hung & Link, 2011). Our goal is to determine the protein's location by tagging the PKHD1L1 gene with the well-known FLAG-tag, which will create a chimeric protein that we can visualize within the cell. Although the presence of a transmembrane domain near the C-terminus (Wu et al., 2019) suggests that the protein may be embedded in a cellular membrane, it is uncertain which membrane this might be. Furthermore, we cannot be certain that the protein is embedded within a membrane until this hypothesis is supported via imaging. We aim to embed the FLAG-tag into the PKHD1L1 gene through co-transfection of mammalian cells with CRISPR and pFETCh vectors. Once successful, we will image the cells and localize the protein using a FLAG-tag antibody. Obtaining insight into the protein's location will allow us to analyze possible functions of PKHD1L1 and compare the gene to other known tumor suppressors.

Materials and Methods

PFETCH Plasmid Engineering

The pFETCh plasmid was engineered using the Mendenhall and Myers Lab Groups' FETCH-seq protocol with the preferred method of designing homology arms with IDT gblocks (Mendenhall & Myers). The pFETCh donor backbone (Mendenhall & Myers, Addgene plasmid

#63934) was digested with BbsI and BsaI enzymes (NE BioLabs) for five hours to ensure complete cutting. BsaI cut at the location of HOM arm 1 (HA1) insertion and BbsI cut at the location of HOM arm 2 (HA2) insertion. The digested pFETCh backbone was ligated with the PCR amplified HOM arms in both 3:1 and 6:1 molar ratios using a single step Gibson Assembly reaction with Gibson Assembly Master Mix (NE BioLabs) for one hour and was then transformed into competent *E. Coli* cells. After a failed transformation in competent cells that are not optimal for large plasmid transformations, the procedure was repeated with high efficiency DH10-beta competent cells (NE BioLabs, #C3019I). The NEB transformation protocol was amended to exclude the suggested serial dilution before plating the competent cells. Each 50µL aliquot of competent cells received either 5 or 15 µL of the pFETCh HOM arm ligation solution. After incubation, the cells were spun down for two minutes at 13,000 RPM and resuspended in 100 µL of NEB 10-beta Stable Outgrowth Medium (NE BioLabs). These 100 µL of competent cells were then plated on LB agar plates containing kanamycin (Fisher BioReagents) to select for cells that had successfully been transformed and were left to incubate at 37ºC overnight.

Following the transformation, colonies from the ligation plates were picked and cultured in Luria Broth with kanamycin. After 18-20 hours of growth in a 37ºC shaking incubator, the cultures were miniprepped with the Wizard *Plus* SV Miniprep DNA Purification System (Promega). The miniprep DNA was subsequently digested with PvuI and ClaI enzymes (NE BioLabs) for four hours. The digested samples were then run on a 0.7% agarose gel in 1X TAE in an electrophoresis chamber at 120V for 45 minutes until the bands had migrated at least halfway across the gel. The gel was stained in ethidium bromide before visualization and the digested bands were compared to a standard DNA ladder (Thermo Scientific GeneRuler 1 kb) that was run in tandem with the digested samples. Proper assembly was evaluated based on the

presence of bands at 300bp, 500 bp, 2.7 Kb, and 3.4 Kb as per the Mendenhall and Myers protocol. The presence of bands at 1.3 Kb or 2.0 Kb rather than 2.7 Kb was used to assess failed or incomplete assembly of the pFETCh vector with both homology arms.

Once gel imaging revealed bands at 300bp, 500 bp, 2.7 Kb, and 3.4 Kb and thus indicated proper plasmid assembly, the DNA samples were sequenced to confirm the complete insertion of both homology arms. Sequencing was performed by Genewiz using the SEQ.HA1, SEQ.P2A, SEQ.HA2 and SEQ.4 forward and reverse primers suggested by the Mendenhall and Myers protocol. Once sequencing confirmed successful pFETCh assembly, the plasmid was maxi-prepped using the GeneJET Plasmid Maxiprep kit (Thermo Fisher Scientific) to amplify the amount of DNA available for future use.

Cell Culture

Kidney 293 cells were grown in MEM/EBSS growth medium (Cytiva) containing 10% fetal bovine serum and 1% penicillin/streptomycin antibiotic solution. The cells were grown in 10cm cell culture dishes and were split 1:3 every 2-3 days upon reaching 70-90% confluency. During splitting, the growth medium was aspirated, the cells were rinsed with sterile phosphate buffer solution (PBS), trypsinized with 0.25% trypsin (Gibco) and then resuspended in complete MEM/EBSS medium. The cells were kept in a humidified 37ºC incubator with 5% CO_2.

Kidney 293 Transfection with pspCas9 and pFETCh Vectors

Cell Plating and Transfection without Antibiotic Selection

Once the 293 cells reached 70-90% confluency in a 10cm cell culture dish, a cell count was conducted to determine the amount of cells needed to seed a 12-well plate to be at 70-90%

confluency during the transfection. A 12-well plate was selected to accommodate poly-L lysine coated glass coverslips to which the cells would adhere during proliferation. On the first day of the transfection, the 12-well plate was seeded and left to incubate overnight to allow the cells to reach the proper confluency. After 18 hours, each of the wells received a solution containing OPTI-MEM (Gibco), P3000 (Invitrogen) and Lipofectamine 3000 reagents (Invitrogen). Per the Lipofectamine 3000 procedure, the amount of Lipo3000 was doubled to optimize transfection efficiency. In order to visually assess efficiency, e-GFP-C2 (0.825 μg) was administered to one well of cells. Two wells received original, unaltered, pspCas9 (Zhang, Addgene plasmid #62988) and pFETCh (Mendenhall & Myers, Addgene plasmid #63934) vectors as a control. Two other wells received engineered pspCas9 pk stop 1 and pFETCh + HA1/HA2. The plate was then left to incubate in the humidified 37ºC incubator for 48 hours prior to imaging and antibody staining.

Transfection with G418 Selection

A second transfection with 293 cells was carried out using G418 (InvivoGen) antibiotic selection. A 12-well plate was seeded to achieve 70-90% confluency at the time of transfection. Due to clumping of the cells and subsequent dense growth after 24 hours, each well was trypsinized, split, and allowed to recover for an additional 48 hours prior to transfection. No poly-L lysine coated glass slips were initially added to the wells. All wells received a solution containing OPTI-MEM (Gibco), P3000 (Invitrogen) and double the amount Lipofectamine 3000 reagents (Invitrogen), as was previously conducted. Wells in row A were not transfected, wells in row B received non-engineered plasmids, and wells in row C were transfected with engineered plasmids. 48 hours after transfection, the pen/strep containing growth medium was removed and replaced. Wells in column 1 received regular MEM/EBSS growth medium with 10% FBS and

1% pen/strep to avoid contamination, wells in column 2 received growth medium with 10% FBS and 200 µg/mL of G418, and wells in column 4 received growth medium with 10% FBS and 500 µg/mL of G418. This growth medium was replaced every 2-3 days. Cells in the 500 µg/mL condition underwent selection for 11 days and had 5 days of recovery in non-antibiotic-containing growth medium whereas cells in the 200 µg/mL condition underwent selection for 14 days and had 2 days of recovery. Selection length was determined by evaluation of cell death in the non-transfected wells, which was considered complete upon 90-95% cell death. After the cells recovered, they were trypsinized, replated onto poly-L lysine coated glass slips, and left to incubate in the humidified 37ºC incubator for 48 hours prior to antibody staining.

Antibody Staining and Imaging

Antibody staining was conducted 48 hours after the transfection without G418 selection and 18 days after the transfection with selection. In both cases, the cells were fixed with 4% formaldehyde diluted in 1X phosphate buffer saline (PBS) for 15 minutes, after which the fixative was aspirated and the cells were washed with 1X PBS three times for five minutes each. After fixation, the cells were blocked in blocking buffer for 60 minutes and then 9A3 mouse monoclonal Flag antibody (Cell Signaling Technology, #8146), diluted 1:1000 in antibody dilution buffer, was applied overnight. The next day, the primary antibody was aspirated and the cells were washed again with 1X PBS three times for five minutes each. Secondary anti-mouse IgG Alexa Fluor® 488 Conjugate fluorescent antibody (Cell Signaling Technology, #4408), diluted 1:1000 in antibody dilution buffer, was then applied for 1-2 hours at room temperature. After the secondary antibody was removed and the slides were rinsed with PBS, the cells were mounted onto glass slides with ProLong® Gold Antifade Reagent with DAPI to allow for nuclear staining and visualization (Cell Signaling Technology, #8961). Both the blocking buffer and the

antibody dilution buffer were prepared according to the Cell Signaling Technology immunocytochemistry protocol.

Once the cells were stained and mounted, the slides were visualized under fluorescent light on an inverted microscope. Images were taken at both 20X magnification and 40X magnification under white light, fluorescent light, and with a blue photo-cube in order to evaluate cell health, FLAG staining, and nuclear staining respectively. Fluorescent images of FLAG staining were taken at a 10 second exposure for both control and experimental cells and nuclear staining images were taken at a 20 second exposure. The FLAG and nuclear-staining images were then overlapped using Advanced SPOT software in order to determine FLAG, and therefore PKHD1L1, localization within the cell relative to the nucleus.

Results

pFETCh Vector Assembly – HOM1

The pFETCh donor backbone (Figure 1) was digested with BsaI (cut sites: 3478, 3503) and BbsI (cut sites: 2455, 2481) in order to insert HOM arm 1 and HOM arm 2 respectively via a four-part ligation.

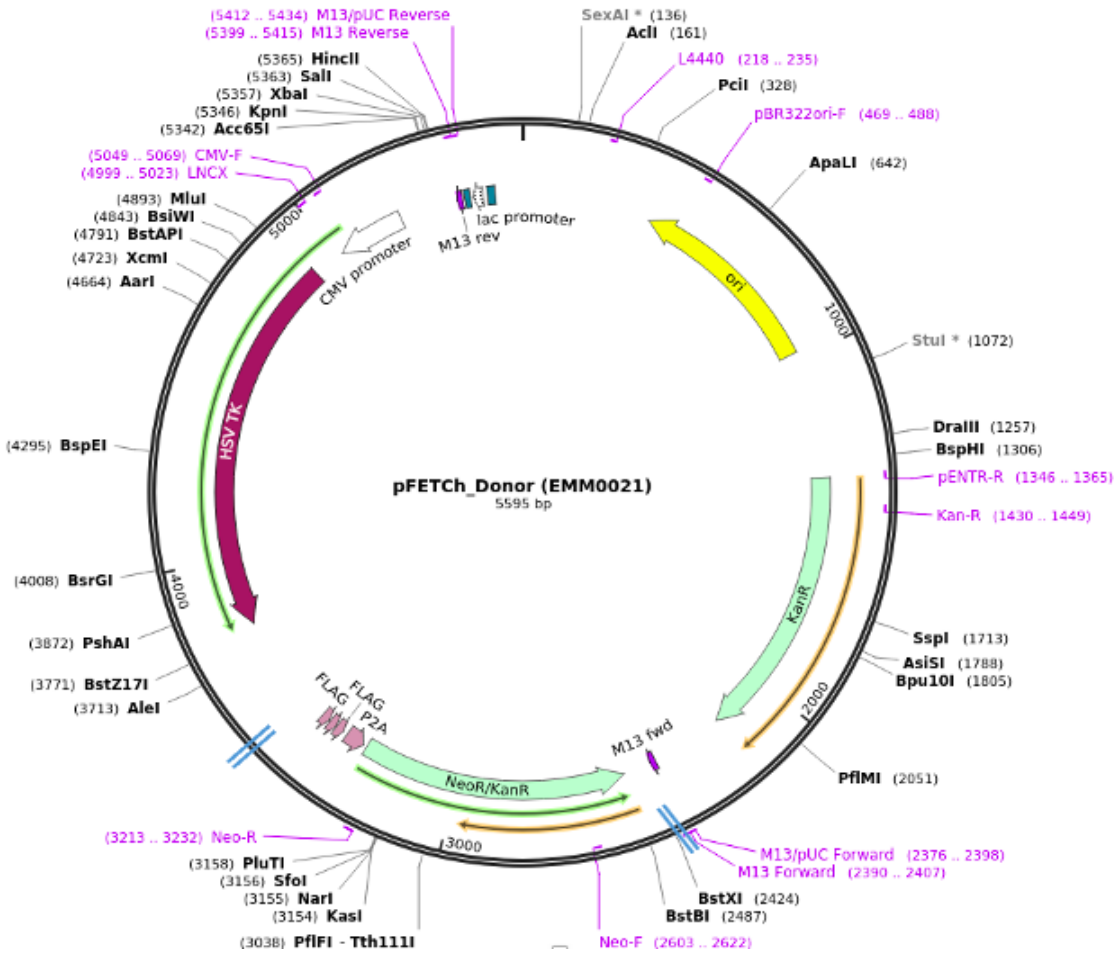

Figure 1. Addgene pFETCh Donor with BsaI (3478, 3503) and BbsI (2455, 2481) cut sites which correspond to HOM1 and HOM2 insertion sites respectively.

Once the plasmid backbone, HOM1 and HOM2 were ligated, the first transformation was attempted using non-high-efficiency competent *E. coli*. After 24 hours of incubation at 37ºC, no colonies had grown indicating either unsuccessful plasmid assembly or inefficient up-take by the cells. Given the large size of the pFETCh donor backbone, the transformation was attempted again with DH10B high-efficiency competent *E. coli* as suggested by the Mendenhall & Myers FETCH-seq protocol. This transformation was marginally more successful than the first, with plates that received spun down ligation mixture (i.e., cells were pelleted and then resuspended in 100 µL of outgrowth medium for a more concentrated solution) growing more colonies than

plates that received the non-spun (i.e. diluted cell/outgrowth medium solution was plated without prior cell pelleting) solution (Table 1).

Table 1. Transformation with DH10B High Efficiency Competent *E. coli.* Ligation mixture was an attempted four part ligation with digested pFETCh donor backbone, HOM1 and HOM2.

Plate	Number of Colonies
3:1 Molar Ratio / 15 µL ligation mixture / No Spin	0
3:1 Molar Ratio / 15 µL ligation mixture / Spin	1
3:1 Molar Ratio / 5 µL ligation mixture / No Spin	0
3:1 Molar Ratio / 5 µL ligation mixture / Spin	29
6:1 Molar Ratio / 15 µL ligation mixture / No Spin	0
6:1 Molar Ratio / 15 µL ligation mixture / Spin	4
Control / 15 µL ligation mixture / No Spin	1
Control / 15 µL ligation mixture / Spin	9

Following the transformation, eight colonies from the 3:1 molar ratio/5µL ligation + spin plate were cultured for miniprep. When the cells from these cultures were spun down prior to isolating the pFETCh plasmid, the cell pellets were quite small. A diagnostic digest was performed with PvuI and ClaI in order to assess whether or not the pFETCh plasmid was successfully engineered and transformed into the cells. According to the Mendenhall and Myers protocol, an empty pFETCh vector should produce bands at 3.4 Kb, **1.3 Kb**, 500 bp and 300 bp. Given the length of each HOM arm (745 bp), successful plasmid assembly should result in bands at 3.4 Kb, **2.7 Kb**, 500 bp and 300 bp. Any other variation of bands may indicate incomplete or unsuccessful assembly of the vector. In the diagnostic digest of the 3:1 molar ratio/5µL ligation + spin miniprep DNA, only culture #1 produced a faint band at 3.4 Kb whereas all other cultures produced no bands due to the low yield of DNA from the miniprep (Figure 2).

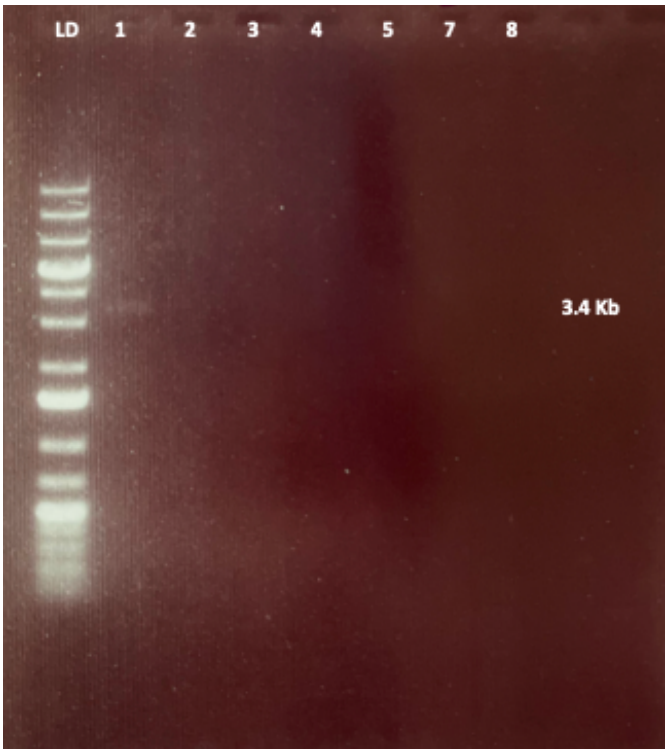

Figure 2. Diagnostic digest with PvuI and ClaI of 5µL miniprep culture DNA (cultures 1-8) from DH10B transformation with pFETCh and attempted HOM1/HOM2 insertion. Successful plasmid assembly should result in bands at 3.4 Kb, 2.7 Kb, 500 bp, and 300 bp. LD = DNA ladder.

In order to amend the previous transformation results, a second transformation was performed using new BbsI enzyme to ensure complete cutting of the plasmid in the hopes of producing better colony ratios between the control and experimental plates. Although this transformation was slightly more successful in regard to the number of colonies that were produced on the experimental plates, the number of colonies on the control plate was significantly higher than expected (Table 2).

Table 2. Second transformation with DH10B Competent *E. coli* and new BbsI enzyme. Ligation mixture was an attempted four part ligation with digested pFETCh donor backbone, HOM1 and HOM2. All tubes were spun down and resuspended in 100 µL of outgrowth medium before plating (spin).

Plate	Number of Colonies
3:1 Molar Ratio / 5 µL ligation mixture / Spin	1
3:1 Molar Ratio / 15 µL ligation mixture / Spin	11
6:1 Molar Ratio / 5 µL ligation mixture / Spin	11
Control / 5 µL ligation mixture / Spin	~500

Cultures were produced using one colony from the 3:1/5µL plate, four colonies from the 3:1/15µL plate, and four colonies from the 6:1/5µL plate. These cultures were mini-prepped (MP) and a diagnostic digest was performed using 5µL of MP DNA. Culture #2 was discarded due to only yielding a very small cell pellet and thus too little DNA to miniprep. The results from this diagnostic digest indicated that MP #4 had a band at ~1.3Kb and therefore contained the empty pFETCh vector (Figure 3A). MP #1 produced no bands and so MP #1 and #4 were discarded. MP #7 produced a band around 2.0 Kb, prompting further investigation into this sample. MP #3, 5, 6, 8 and 9 produced very faint bands at 3.4 Kb, 500 bp and 300 bp (Figure 3A).

In order to further investigate MP samples #3, 5, 6, 7, 8 and 9, a new diagnostic digest was performed using 15µL of MP DNA in the hopes of producing brighter bands to see if any other samples had a band around 2.0 or 2.7 Kb. This digest confirmed our prior observations that MP #3, 5, 6, 8 and 9 only had bands at 3.4 Kb, 500 bp, and 300 bp. MP #7 still produced a strong additional band at 2.0 Kb (Figure 3B). In order to determine whether or not the HOM arms had been successfully inserted into the plasmid, MP #7 was sequenced using both forward and

reverse primers for HOM1 and HOM2. The sequencing results indicated that HOM1 had been successfully inserted, but that HOM2 was absent from the engineered pFETCh plasmid.

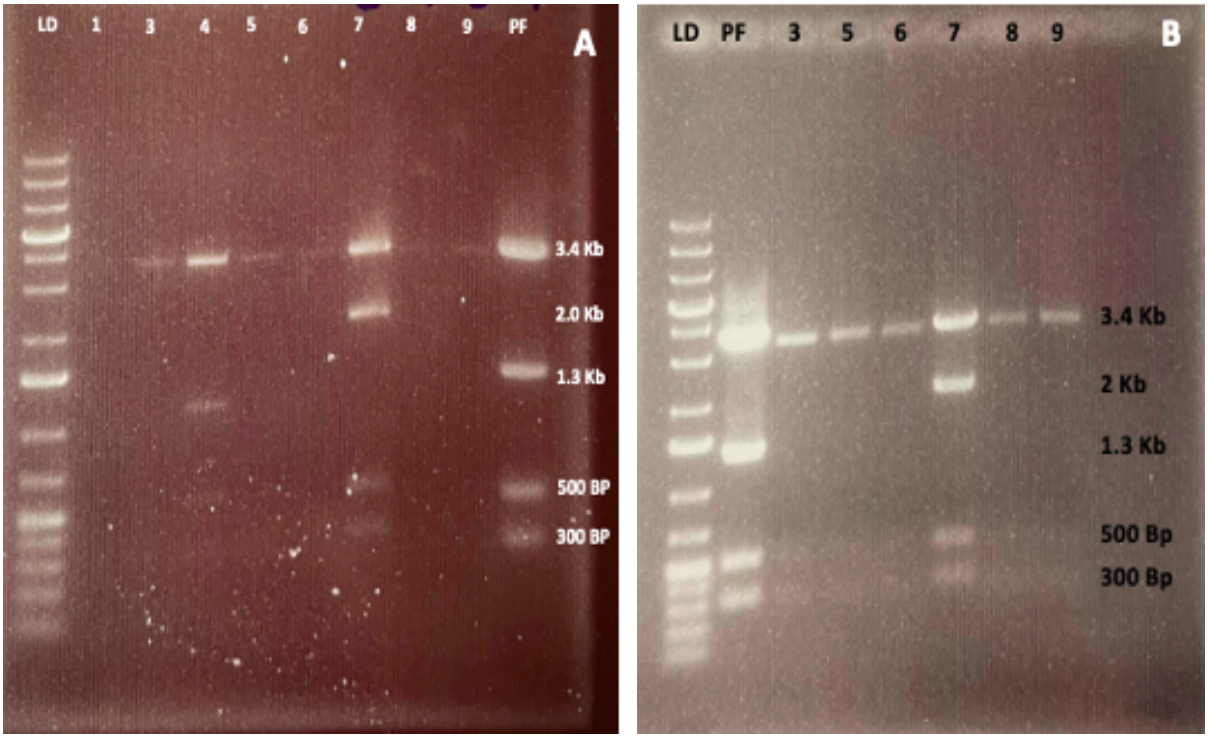

Figure 3. Diagnostic digest with PvuI and ClaI of pFETCh (PF) and miniprep culture DNA. A) 5µL MP DNA (cultures 1, and 3-9). B) 15µL of miniprep culture DNA (cultures 3 and 5-9). MP DNA was taken from DH10B transformation with pFETCh and attempted HOM1/HOM2 insertion. Successful plasmid assembly should result in bands at 3.4 Kb, 2.7 Kb, 500 bp, and 300 bp. LD = DNA ladder.

pFETCh Vector Assembly – HOM1 + HOM2

In order to tag PKHD1L1, both HOM arms must be fully inserted into the pFETCh plasmid. Therefore, the Mendenhall and Myers FETCH-seq protocol was repeated, this time using the previously engineered pFETCh plasmid MP #7 containing HOM1 in the backbone. New HOM2 PCR solutions were prepared to ensure maximum efficiency. The PCR concentrations were re-quantified with a nanodrop, and significantly lower concentrations were recorded than the assumed working concentrations for the previous transformations. The molar ratio was adjusted accordingly, likely more accurately representing a 3:1 ratio of PCR product to

pFETCh backbone, and the new ligation mixture was transformed into DH10B high efficiency *E. coli.* This transformation was significantly more successful than the previous attempts. Experimental plates grew colonies that were too numerous to count, and only one out of two control plates grew colonies (Table 3).

Table 3. Third transformation with DH10B Competent *E. coli*. Inserted plasmid already contained HOM1 and HOM2 was the attempted insertion in the current ligation. TNTC = too numerous to count.

Plate	Number of Colonies
3:1 Molar Ratio / 5 µL ligation mixture / Spin	TNTC
3:1 Molar Ratio / 15 µL ligation mixture / Spin	TNTC
Control / 5 µL ligation mixture / Spin	0
Control / 15 µL ligation mixture / Spin	5

From this transformation, six cultures were prepared and mini-prepped. The subsequent diagnostic digest presented bands at 3.4Kb, 2.7Kb, 500bp and 300bp for each culture, indicating successful assembly in all of the evaluated samples (Figure 5). MP #2, 3, and 5 were sequenced due to having the highest concentrations upon nanodrop quantification (31.0 ng/µL, 148.5 ng/µL and 28.2 ng/µL respectively). Sequencing indicated that MP #2 and #5 contained successfully assembled pFETCh with both HOM1 and HOM2 fully inserted. MP #3 was shown to only have incorporated 625 out of HOM2's 745 base pairs and was thus discarded.

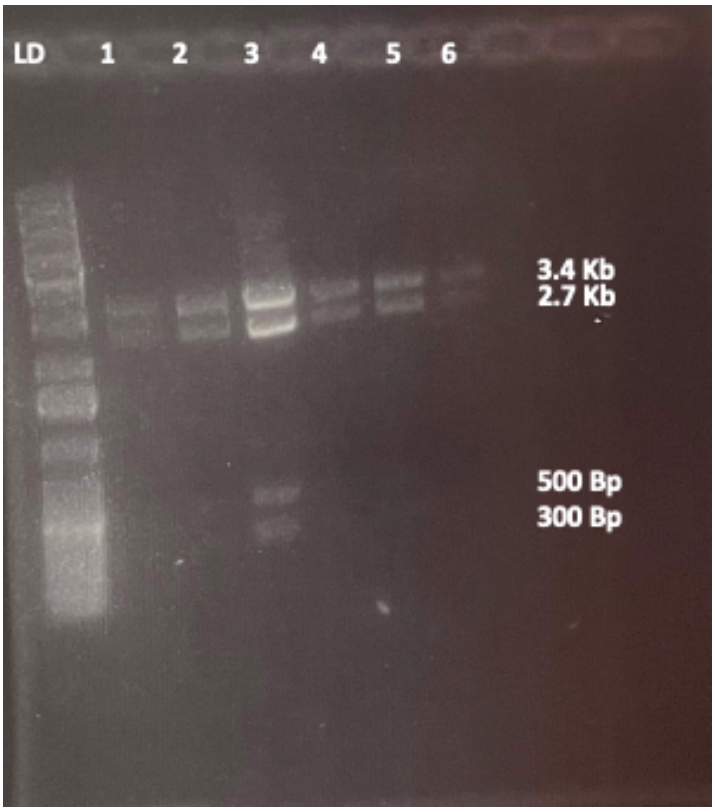

Figure 5. Diagnostic digest with PvuI and ClaI of 5µL of miniprep culture DNA (cultures 1-6) from DH10B transformation with pFETCh + HOM1 and attempted HOM2 insertion. Successful plasmid assembly should result in bands at 3.4 Kb, 2.7 Kb, 500 bp, and 300 bp. LD = DNA ladder.

Visualization of PKHD1L1 via FLAG-tagging

Once MP #5 was maxi-prepped and sufficient DNA was produced, kidney 293 cells were co-transfected with engineered pFETCh and CRISPR/Cas9 (produced by Sydney Nyquist and Dr. Lina Yoo) plasmids. With pspCas9 targeting the PKHD1L1 stop codon, our hope was that natural DNA repair mechanisms would result in the insertion of the FLAG-tag into the end of the gene via a crossing-over event. The FLAG portion of the resulting chimeric protein is what we attempted to visualize in order to assess PKHD1L1 localization within the cell. In order to assess transfection efficiency, and therefore the likelihood that recombination occurred given plasmid uptake by the cells, one well of cells was transfected with eGFP-C2. Visualization of the eGFP-C2 fluorescence indicated that the transfection efficiency was around 45% (Figure 6).

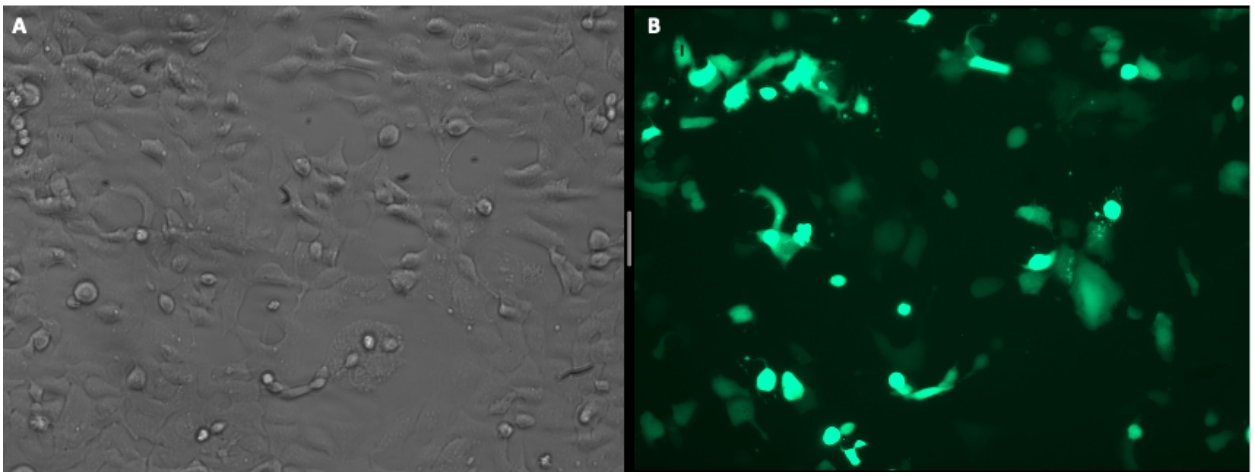

Figure 6. eGFP-C2 staining of kidney 293 cells. A) White light image at 20X magnification. B) Fluorescent visualization of eGFP-C2 at 20X magnification. Transfection efficiency is ~45%.

Control wells were transfected with original pspCas9 and pFETCh vectors in order to assess background staining whereas experimental wells were transfected with the previously engineered vectors. Antibody staining with mouse 9A3 Flag antibody and secondary anti-mouse antibody revealed that although there was a significant amount of background staining in the control cells, we were able to observe increased fluorescence in some experimental cells (Fig. 7, Fig. 8). Comparison of white light images to fluorescent images of cells transfected with engineered plasmids showed that the heavily fluorescing cells were healthy and stretched out, indicating that the fluorescence was not due to abnormal antibody staining in unhealthy cells (Figure 9).

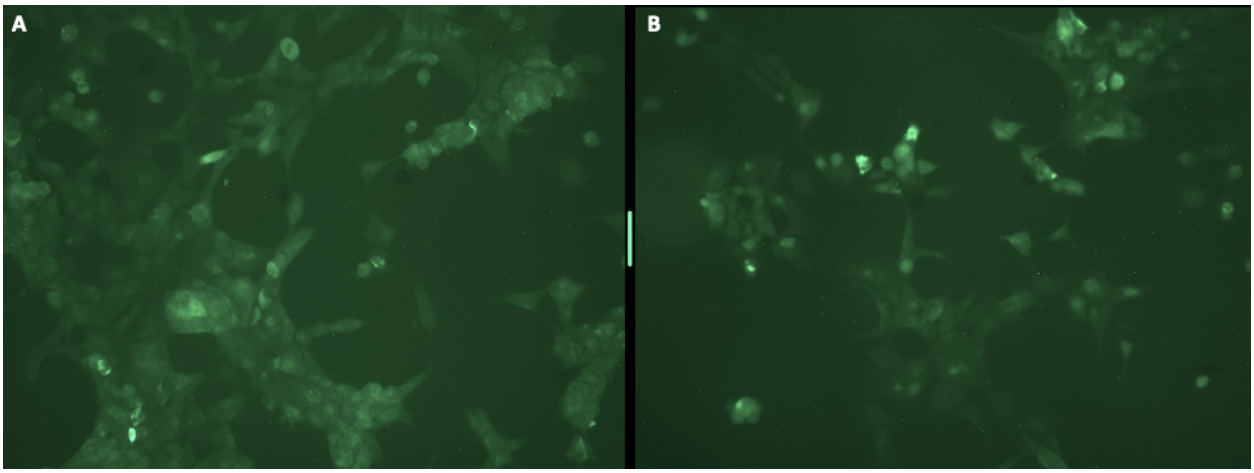

Figure 7. Visualization of FLAG-tag on PKHD1L1 via antibody staining. A) control, 20X magnification, 10s exposure. B) FLAG-tagged PKHD1L1, 20X magnification, 10s exposure.

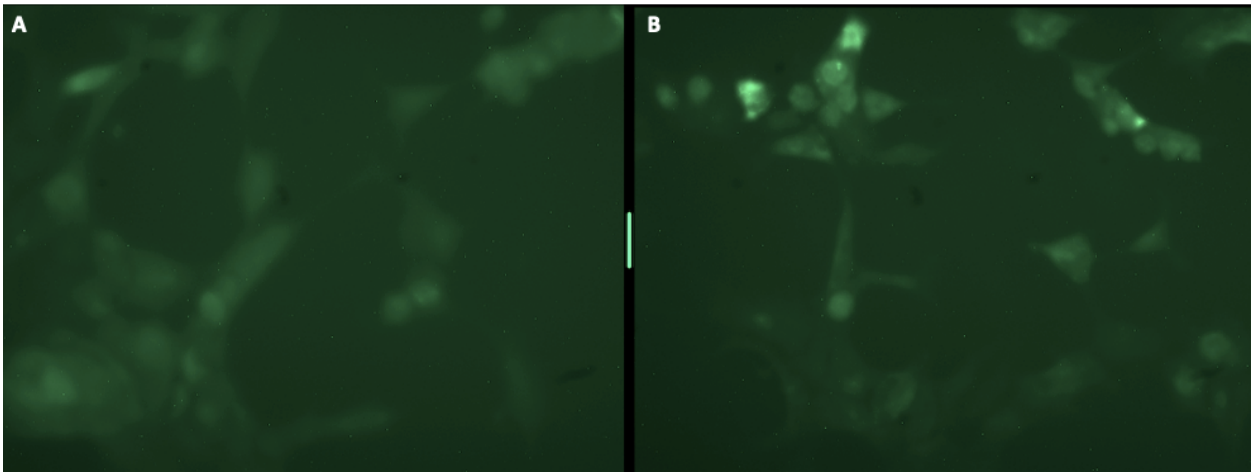

Figure 8. Visualization of FLAG-tag on PKHD1L1 via antibody staining. A) control, 40X magnification, 10s exposure. B) FLAG-tagged PKHD1L1, 40X magnification, 10s exposure.

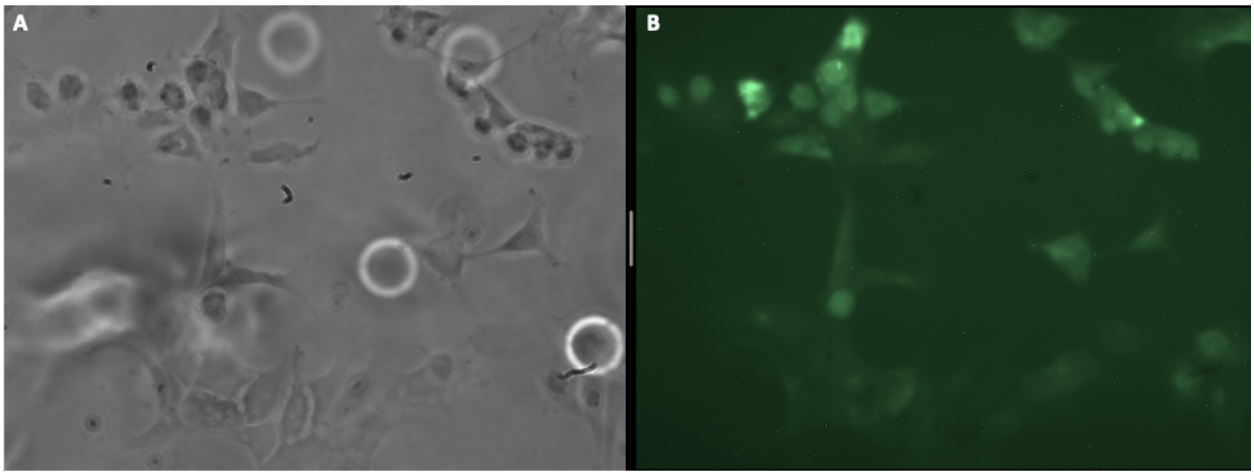

Figure 9. Visualization of FLAG-tag on PKHD1L1 via antibody staining. A) FLAG-tagged PKHD1L1, white light, 40X magnification. B) FLAG-tagged PKHD1L1, 40X magnification, 10s exposure.

Our second transformation with G418 antibiotic selection provided conflicting results regarding PKHD1L1 localization. Cells that received 200 µg/mL of G418 appeared to have undergone a gentler selection, resulting in more cells to visualize compared to the 500 µg/mL condition. In spite of the differences in cell density, both conditions had sufficient cells to visualize and did not differ in regard to fluorescence. Some images of the cells indicated that levels of fluorescence did not appear to be significantly different (Figure 10). However, in other images with increased cell density, recombinant cells do appear to be fluorescing at a higher level compared to control cells (Figure 11). When nuclear staining images were overlapped with images of FLAG visualization, the antibody staining appeared to be mostly cytoplasmic. Given that the FLAG-tag was embedded into the PKHD1L1 gene, resulting in a chimeric protein, these results indicate that PKHD1L1 may be cytoplasmic (Figure 12). Some of the staining in these comparative images does appear to occur in unhealthy cells (Figure 13), but the majority of the cells are healthy and stretched out indicating that the antibody staining is not abnormal in those cells and that fluorescence reflects PKHD1L1 localization.

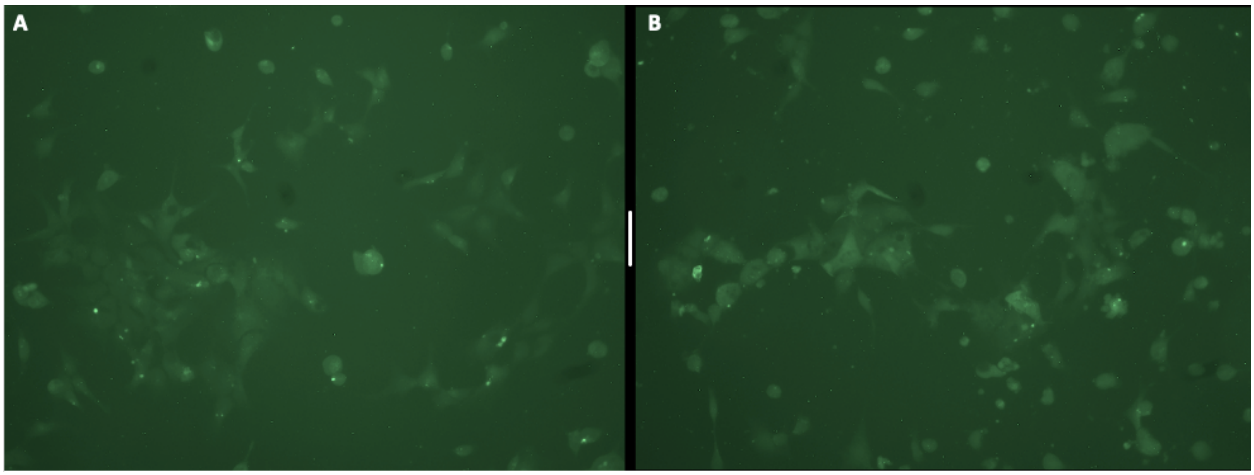

Figure 10. Visualization of FLAG-tag on PKHD1L1 via antibody staining in G418 (200µg/mL) selected cells. A) control, 20X magnification, 10s exposure. B) FLAG-tagged PKHD1L1, 20X magnification, 10s exposure.

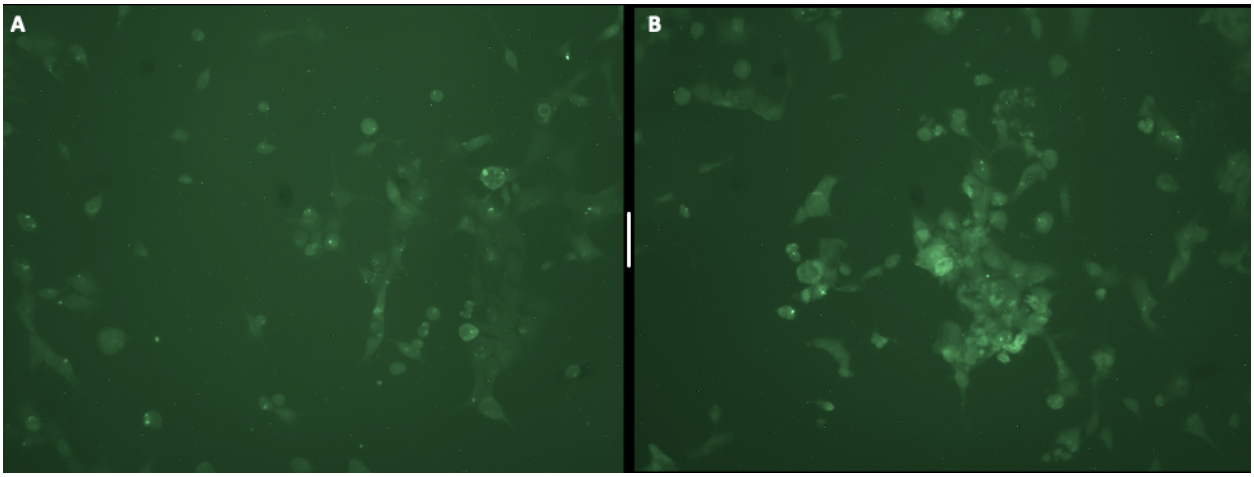

Figure 11. Visualization of FLAG-tag on PKHD1L1 via antibody staining in G418 (200µg/mL) selected cells. A) control, 20X magnification, 10s exposure. B) FLAG-tagged PKHD1L1, 20X magnification, 10s exposure.

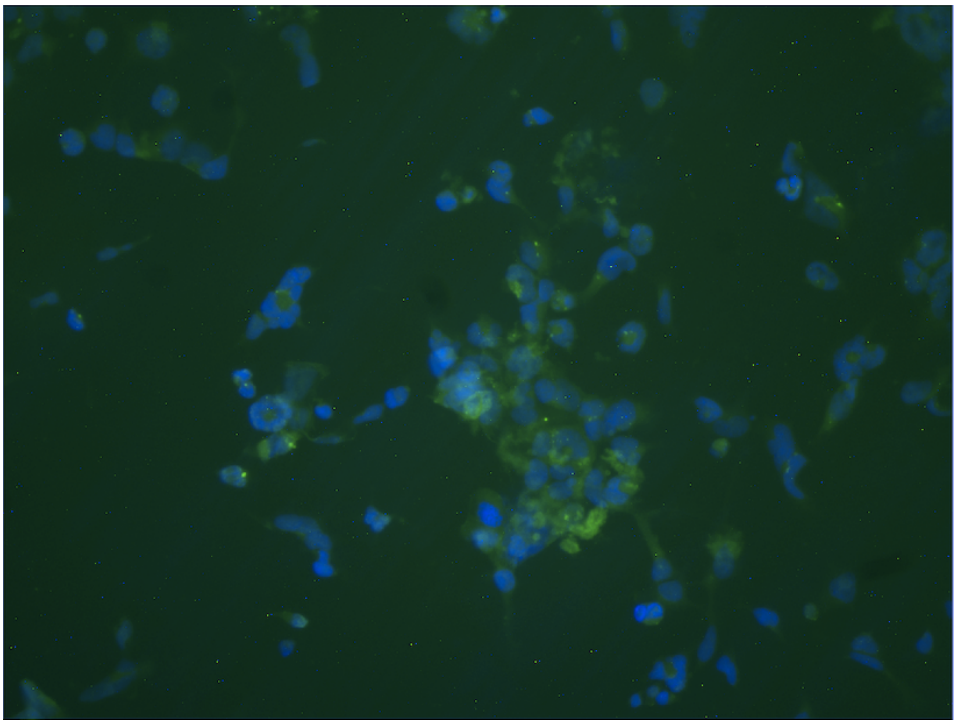

Figure 12. Visualization of nucleus (blue) and FLAG-tag (green) on PKHD1L1 via antibody staining in G418 (200µg/mL) selected cells. Images were taken at 20X magnification and 10s exposure and overlapped using Advanced SPOT software.

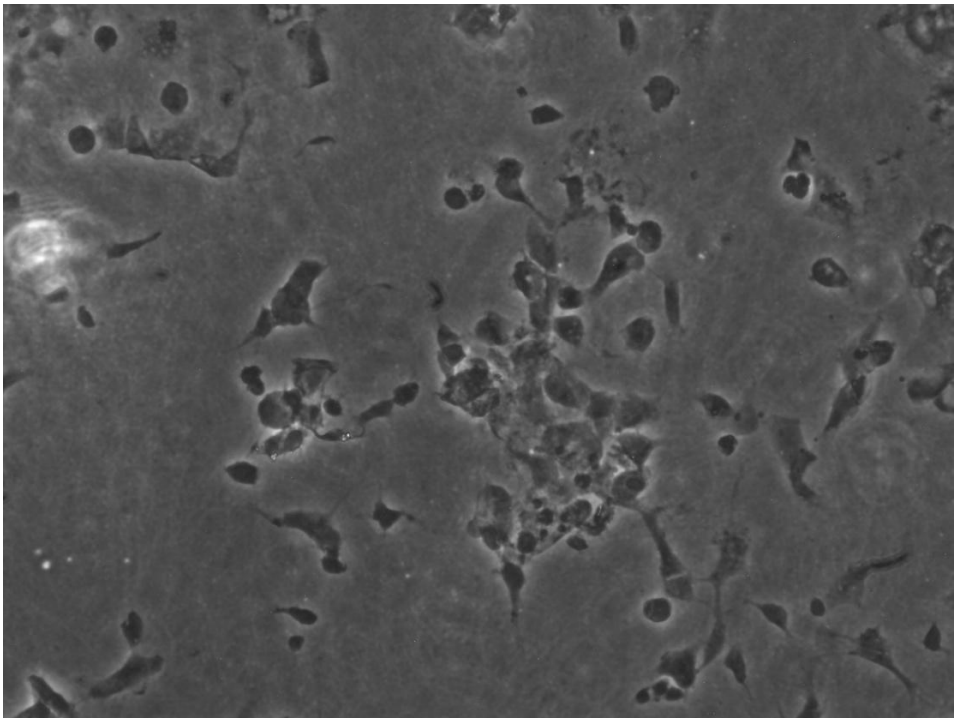

Figure 13. White light image of G418 (200µg/mL) selected cells in figure 13. Image was taken at 20X magnification.

Discussion

Engineering the pFETCh Plasmid

The findings in this study illustrate that while it is possible to assemble the pFETCh plasmid via the Mendenhall & Myers FETCH-seq protocol, the process can be difficult. Given the failure of our first transformation with competent *E. coli* that are not suitable for large vectors, one can conclude that high efficiency *E. coli* are the most appropriate to use in this assembly. Furthermore, due to the slow growth of the bacteria during the transformation, it appears that the pFETCh plasmid may be slightly harmful to the cells. Therefore, longer incubation times were required in order to obtain an appropriate bacterial load for plasmid purification. We also found that ensuring a proper 3:1 molar ratio of PCR plasmid to digested pFETCh backbone was essential for proper plasmid assembly. During our first transformation with DH10B high efficiency *E. coli*, only HOM1 was successfully inserted into the vector. This result appears to have been due to an improper molar ratio during the ligation procedure. The molar ratio was originally calculated using a working concentration based on the original pFETCh donor concentration. However, upon re-quantification of the digested plasmid, we found that the concentration was roughly 30-fold lower than expected. The digested vector, compared to the original plasmid, appears to have undergone degradation leading to a significantly lower concentration than expected. Therefore, quantification both before and after digestion are necessary in order to ensure that a correct molar ratio is calculated for the ligation. Once the molar ratio was corrected, we observed an improved ratio of colonies on the experimental vs control transformation plates.

In addition to increasing bacterial incubation times and ensuring proper ligation ratios, we found Sanger sequencing to be another essential factor during plasmid assembly. Although a

diagnostic digest evaluated via gel electrophoresis is appropriate for determining whether or not the necessary bands are visible at 3.4 Kb, 2.7 Kb, 500 bp, and 300bp, sequencing is necessary in order to determine whether or not the homology arms have been fully inserted. We observed one homology arm that was incompletely inserted for unknown reasons, but via Sanger sequencing we were able to rule out this sample prior to 293 transfection. Ensuring complete HOM arm insertion is necessary due to DNA repair mechanisms relying on nearby homology sequences when double stranded breaks occur. Crossing over events between the "break", a cut carried out by pspCas9 near the stop codon, and the homology arms on the pFETCh vector allow the FLAG-tag and neomycin resistance genes from the plasmid to be inserted into the PKHD1L1 gene. If the homology arms are not completely inserted, the chances of the crossing over event occurring may be decreased due to less sequence similarities being recognized by the DNA repair mechanisms.

293 Transfection and G418 Selection

Given the different transfection conditions attempted in this study, we were able to conclude that co-transfection with the pFETCh and pspCas9 plasmids is possible and optimal with 200µg/mL G418 antibiotic selection. The first transfection was attempted with double the amount of Lipofectamine 3000, an alternative proposed by the Invitrogen procedure, and no antibiotic selection due to concerns about the plasmids causing harm to the cells. The amount of Lipofectamine 3000 used appeared to be problematic as it caused a large amount of cell death, indicating that the original suggestion of a lower amount may be more appropriate for this transfection as long as the transfection efficiency is not significantly compromised. The second transfection was conducted using antibiotic selection with G418. In this transfection, we found

that 200µg/mL of G418 over a period of 14 days and 2 days of recovery resulted in a better selection compared to cells that were selected with 500µg/mL of antibiotic, which required 5 days to recover and still resulted in a lower confluency. Therefore, the lower antibiotic concentration recommended by previous literature (Chen et al., 2003; Hennen et al., 2013) appeared to more gently select for the plasmid-containing cells without being overly harmful.

PKHD1L1 Visualization via FLAG-tag Antibody Staining

The results of this study are inconclusive in showing whether or not a FLAG-tag can be introduced into the PKHD1L1 gene in order to visualize the protein product in the cell via antibody staining. The fluorescent imaging of control and recombinant cells in the non-selection transfection were not drastically different, but there was a notable enough difference to suggest that recombinant cells were fluorescing at a higher level. The cells that were fluorescing in these images were also healthy and spread out, indicating that the higher level of fluorescence may be due to the FLAG-tag rather than irregular staining of unhealthy cells. However, imaging of cells in the G418 selection transfection showed very similar staining in both control and recombinant cells. There was a significant amount of background staining occurring in the control cells, indicating that the fluorescent anti-mouse antibody may have bound non-specifically to other cell components.

In addition to the secondary antibody potentially binding non-specifically, Sydney Nyquist found in her Senior Research that PKHD1L1 expression in kidney 293 cells appears to be low. Her data indicate that PKHD1L1 is in fact expressed in these cells, which is promising in suggesting that we can tag and visualize the protein, but this expression is much lower than the levels of beta-actin, a housekeeping gene that functions as a control. These findings, taken in

consideration with the fluorescent imaging, suggest that since expression levels are low, we must look for small differences between the control and recombinant cells. Finding such miniscule differences is further complicated by the significant background staining that occurred. Therefore, although our data indicate that the FLAG-tag can be visualized in some cells, further work must be done to reduce background staining in order to see the faint staining we are looking for.

Future Visualization of PKHD1L1 and Possible Implications

Although we were not able to confidently localize the PKHD1L1 protein in this study, the groundwork laid here has shown promising results for refining our methods in order to determine the protein's location in the future. Our primary focus was to determine whether or not the FLAG-tag could be used to visualize the PKHD1L1 gene product and although 293 staining was contradictory, our data indicate that if background staining can be reduced, slight differences in fluorescence may be observed. Future studies should include further staining in order to overlap FLAG-tag staining with organelle staining in order to determine to which organelles the protein may be localizing. Previous research suggests that the PKHD1L1 protein is large, extracellular, and has a single transmembrane domain near the C-terminus, although these statements have not been supported (Wu et al., 2019). If this localization is supported in the future, it will be necessary to investigate the potential functions of PKHD1L1 as a trans-membrane protein. Furthermore, it will be necessary to determine whether the protein is embedded in the outer cell membrane, the nuclear membrane, or another membrane. As a potential membrane protein, PKHD1L1 could be implicated in a variety of processes involved in cell survival, proliferation, gene regulation/transcription, apoptosis, invasion, metastasis, and

activation of downstream signaling pathways. Integrins, cytokine receptors, chemokine transmitters, and receptor tyrosine kinases are all involved in these processes and would be avenues of further research should PKHD1L1 be found to be a transmembrane protein (Kampen, 2011).

Aside from investigating the potential transmembrane location of the PKHD1L1 protein, future studies should also investigate whether or not the protein localizes to the nucleus at all. Given the previously discussed functions of caretaker proteins, should the protein be located in the nucleus, it may play a role similar to BRCA1 and BRCA2 in DNA repair, DNA recombination, checkpoint control in the cell cycle, transcription, and preserving chromosome structure (Venkitaraman, 2002). Alternatively, as a caretaker, PKHD1L1 may be implicated in regulating cell division and apoptosis (Kinzler and Vogelstein, 1997). There is some support for PKHD1L1 functioning as a caretaker protein given its proposed interactions with other proteins and their observed functions within the cell. The STRING interaction network suggests that PKHD1L1 appears to interact with various proteins including CACHD1 and PYROXD1 (PKHD1L1 protein (human) - STRING interaction network). CACHD1 has been observed to regulate voltage gated calcium channels (Cottrell et al., 2018), which are implicated in cell proliferation, apoptosis, metastasis and initiation of mitosis (Phan et al., 2017). Furthermore, studies have shown that genes related to voltage-gated calcium channels were under-expressed in various epithelial cancers, including breast, lung and kidney (Phan et al., 2017), indicating that if PKHD1L1 is interacting with these proteins, such as CACHD1, then it may be further contributing to the development and progression of cancer when mutated.

The second proposed protein interaction that may indicate that PKHD1L1 has caretaker functions is its interaction with PYROXD1. PYROXD1 is a protein that is implicated in the

cellular response to oxidative stress and cellular respiration (PKHD1L1 protein (human) - STRING interaction network; Saha et al., 2018). Previous studies have observed that when the PYROXD1 protein was deficient in cells, cellular proliferation, differentiation, and migration were impaired (Saha et al., 2018). These findings suggest that if PKHD1L1 interacts with the PYROXD1 protein, it may help regulate these cellular processes. In regard to cellular respiration, PYROXD1 has not been observed to localize to the mitochondria, although it appears to have a role in cellular respiration since it is decreased when the protein is deficient (Saha et al., 2018). For this reason, future studies on PKHD1L1 should also explore whether or not the protein product localizes to or near the mitochondria, since its proposed interaction with PYROXD1 suggests that it may be involved in cellular respiration.

Should PKHD1L1 be implicated in cellular respiration or other mitochondrial functions, its impact on cancer development and progression could be approached from another angle. The mitochondria regulates cellular energetics, which are commonly disrupted in cancerous cells. This organelle participates in a host of cellular functions including not only providing energy, but regulating apoptosis and signaling to the rest of the cell when homeostasis is disrupted (Wallace et al., 2010; Galluzzi et al., 2012). Based on the mitochondria's participation in these pathways, it is clear how disrupting its function can lead to metabolic disorders, including cancer. Furthermore, mitochondrial disruption has been found to trigger cytosolic signaling pathways that can eventually lead to altered gene expression in the nucleus (Hsu et al., 2016). This observation is particularly relevant given Wang et al.'s findings that when PKHD1L1 was mutated at a single nucleotide, its expression was downregulated (Wang et al., 2020). If PKHD1L1 were implicated in mitochondrial function, it is possible that its mutation might trigger a cytosolic signaling pathway leading back to nuclear gene expression. This suggestion is

also supported by the finding from the same research group that the SNP in mutated PKHD1L1 associated with lung adenocarcinomas occurs at rs768349010, which correlates to location 109445307 on chromosome 8 of the PKHD1L1 gene, and results in a code switch from AGU to GGU (U.S. National Library of Medicine; Wang et al., 2020). This change in a single nucleotide results in a code switch from serine to glycine, meaning that serine, a polar amino acid that is capable of hydrogen bonding, is switched out for glycine, a small, non-polar amino acid. This missense mutation could likely result in protein misfolding that may cause aberrant functioning and incorrect association with other protein partners. Taking these findings into account, if the PKHD1L1 protein is mutated, resulting in an incorrectly functional protein, that protein may not associate with its partners such as PYROXD1 correctly. This compromised interaction could in turn result in signaling pathways that downregulate the expression of PKHD1L1 in the nucleus as has been observed in previous studies (Grossman et al., 2016; Wang et al., 2020) and thus may limit its ability to function as a tumor suppressing gene.

Concluding remarks

Given the previous research on PKHD1L1 and its potential location within the cell, it is possible to hypothesize a myriad of hypothetical functions. Although we can propose functions, the next step in researching this gene is pinpointing its location in order to further explore its role within a specific organelle, membrane, or compartment. Given that PKHD1L1 is highly mutated in epithelial cancers and is downregulated in cancerous cells, the gene appears to have tumor suppressing qualities. However, until we can propose a more focused function of the protein, the way PKHD1L1 may function as an anti-oncogene remains uncertain. The data presented in this study suggest that localizing the protein via antibody staining of the FLAG-tag may be a viable

route to continue researching if the methodology can be improved to reduce background staining. Given the seemingly essential function of PKHD1L1 in healthy tissues, future studies in this field will continue to provide groundbreaking insight into the progression and development of epithelial cancers.

Acknowledgements

I would like to acknowledge Dr. Lina Yoo for allowing me to work on this project with her and for being an invaluable mentor during my time at Denison. I would also like to thank my lab partner, Sydney Nyquist, for her help and constant patience in the lab, as well as my second advisor, Dr. Jeff Thompson, for challenging me to dig deeper into my research and for teaching me about genetics. Finally, I would also like to thank the Biology Department for providing me with a great education in this field and the Lisska Center for providing funding for this project. This work would not have been possible without all of the people who helped me through the research process.

References

Cell Signaling Technology. *Anti-mouse IgG (H+L), F(ab')2 Fragment (Alexa Fluor® 488 Conjugate.* https://www.cellsignal.com/products/secondary-antibodies/anti-mouse-igg-h-l-f-ab-2-fragment-alexa-fluor-488-conjugate/4408.

Cell Signaling Technology. *DYKDDDDK Tag (9A3) Mouse mAb (Binds to same epitope as Sigma's Anti-FLAG® M2 Antibody)*. https://www.cellsignal.com/products/primary-antibodies/dykddddk-tag-9a3-mouse-mab-binds-to-same-epitope-as-sigma-s-anti-flag-m2-antibody/8146.

Centers for Disease Control and Prevention. *USCS Data Visualizations - CDC*. Centers for Disease Control and Prevention. https://gis.cdc.gov/Cancer/USCS/DataViz.html.

Chen, Q., Behar, K. L., Xu, T., Fan, C., & Haddad, G. G. (2003). Expression of Drosophila trehalose-phosphate synthase in HEK-293 cells increases hypoxia tolerance. *The Journal of biological chemistry*, *278*(49), 49113–49118. https://doi.org/10.1074/jbc.M308652200

Cottrell, G. S., Soubrane, C. H., Hounshell, J. A., Lin, H., Owenson, V., Rigby, M., Cox, P., Barker, B., Ottolini, M., Ince, S., Bauer, C., Perez-Reyez, E., Patel, M., Steven, E., Stephens, G. J. (2018). CACHD1 is an α2δ-Like Protein That Modulates Ca_V3 Voltage-Gated Calcium Channel Activity. *The Journal of Neuroscience*, *38*(43), 9186. doi: 10.1523/JNEUROSCI.3572-15.2018

Erdman, V. V., Karimov, D. D., Nasibullin, T. R., Timasheva, I. R., Tuktarova, I. A., & Mustafina, O. E. (2017). The role of Alu polymorphism of PLAT, PKHD1L1, STK38L, and TEAD1 genes in development of a longevity trait. *Advances in Gerontology*, *7*(2), 107–113. https://doi.org/10.1134/s2079057017020059

Galluzzi, L., Kepp, O., & Kroemer, G. (2012). Mitochondria: master regulators of danger signaling. *Nature reviews. Molecular cell bio3ogy*, *13*(12), 780–788. https://doi.org/10.1038/nrm3479

Giovannucci, E. & Willett, W. C. (1994) Dietary Factors and Risk of Colon Cancer, *Annals of Medicine*, 26:6, 443-452, DOI:10.3109/07853899409148367

Grossman, R. L., Heath, A. P., Ferretti, V., Varmus, H. E., Lowy, D. R., Kibbe, W. A., Staudt, L. M. (2016). Toward a Shared Vision for Cancer Genomic Data. *New England Journal of Medicine,* 375:12, 1109-1112

Hennen, S., Wang, H., Peters, L., Merten, N., Simon, K., Spinrath, A., Blättermann, S., Akkari,

R., Schrage, R., Schröder, R., Schulz, D., Vermeiren, C., Zimmermann, K., Kehraus, S., Drewke, C., Pfeifer, A., König, G. M., Mohr, K., Gillard, M., Müller, C. E., Lu, Q., Gomeza, J., Kostenis, E. (2013). Decoding signaling and function of the orphan G protein-coupled receptor GPR17 with a small-molecule agonist. *Science signaling*, *6*(298), ra93. https://doi.org/10.1126/scisignal.2004350

Hogan, M. C., Griffin, M. D., Rossetti, S., Torres, V. E., Ward, C. J., & Harris, P. C. (2003). PKHDL1, a homolog of the autosomal recessive polycystic kidney disease gene, encodes a receptor with inducible T lymphocyte expression. *Human Molecular Genetics*, 12(6), 685–698. https://doi.org/10.1093/hmg/ddg068

Hsu, C. C., Tseng, L. M., & Lee, H. C. (2016). Role of mitochondrial dysfunction in cancer progression. *Experimental biology and medicine (Maywood, N.J.)*, *241*(12), 1281–1295. https://doi.org/10.1177/1535370216641787

Hung, M.-C., & Link, W. (2011). Protein localization in disease and therapy. *Journal of Cell Science*, *124*(20), 3381–3392. https://doi.org/10.1242/jcs.089110

Kampen, K.R. (2011). Membrane Proteins: The Key Players of a Cancer Cell. *The Journal of Membrane Biology,* 242, 69–74. https://doi.org/10.1007/s00232-011-9381-7

Kinzler, K. W., & Vogelstein, B. (1996). Lessons from Hereditary Colorectal Cancer. *Cell*, *87*(2), 159–170. https://doi.org/10.1016/s0092-8674(00)81333-1

Kinzler, K., Vogelstein, B. (1997). Gatekeepers and caretakers. *Nature* 386, 761–763. https://doi.org/10.1038/386761a0

Knudson, A. G. (1993). Antioncogenes and human cancer. *Proceedings of the National Academy of Sciences*, *90*(23), 10914–10921. https://doi.org/10.1073/pnas.90.23.10914

Knudson, A.G. (1996). Hereditary cancer: Two hits revisited. *J Cancer Res Clin Oncol* 122, 135–140. https://doi.org/10.1007/BF01366952

Lian, P. W., Fu, Y. L., Li, A., Dai, B. Z., Ding, Z. W., Li, L., & Wu, G. Q. (2011). *Xi bao yu fen zi mian yi xue za zhi = Chinese journal of cellular and molecular immunology*, *27*(1), 78–81.

Mendenhall and Myers Lab Groups HudsonAlpha Institute for Biotechnology FETCh-seq Protocols. *Scheme of Design of Vectors and Establishment of Mammalian Cell Lines With Flag Tagged Endogenous Proteins For ChIP-Seq*.

National Cancer Institute. *Cancer Classification*. National Institutes of Health.

National Cancer Institute. *PKHD1L1*. Genomic Data Commons Data Portal. https://portal.gdc.cancer.gov/genes/ENSG00000205038.

New England BioLabs. (2014). High efficiency transformation protocol using neb 10-beta competent E. coli (C3019I). *Protocols.io*. doi:10.17504/protocols.io.cf5tq5

Phan, N.N., Wang, C., Chen, C., Sun, Z., Lai, M., & Lin, Y. (2017). Voltage-gated calcium channels: Novel targets for cancer therapy. *Oncology Letters*, 14, 2059-2074. https://doi.org/10.3892/ol.2017.6457

PKHD1L1 protein (human) - STRING interaction network. (n.d.). https://www.string-db.org/cgi/network?taskId=bezm1Nw0FtS0&sessionId=bhLQohg85MRa

Ran, F. A., Hsu, P. D., Wright, J., Agarwala, V., Scott, D. A., & Zhang, F. (2013). Genome engineering using the CRISPR-Cas9 system. *Nature protocols*, *8*(11), 2281–2308. https://doi.org/10.1038/nprot.2013.143

Saha, M., Reddy, H. M., Salih, M. A., Estrella, E., Jones, M. D., Mitsuhashi, S., Cho, K., Suzuki-Hatano, S., Rizzo, S., Hamad, M., Mukhtar, M., Hamed, A., Elseed, M., Lek, M., Valkanas, E., MacArthur, D., Kunkel, L., Pacak, C., Draper, I., Kang, P. (2018). Impact of PYROXD1 deficiency on cellular respiration and correlations with genetic analyses of limb-girdle muscular dystrophy in Saudi Arabia and Sudan. *Physiological Genomics*, 50(11), 929–939. https://doi.org/10.1152/physiolgenomics.00036.2018

Savic, D., Partridge, E. C., Newberry, K. M., Smith, S. B., Meadows, S. K., Roberts, B. S., Mackiewicz, M., Mendenhall, E. M., & Myers, R. M. (2015). CETCh-seq: CRISPR epitope tagging ChIP-seq of DNA-binding proteins. *Genome research*, *25*(10), 1581–1589. https://doi.org/10.1101/gr.193540.115

Sharan, S. K., Morimatsu, M., Albrecht, U., Lim, D.-S., Regel, E., Dinh, C., Sands, A., Eichele, G., Hasty, P., Bradley, A. (1997). Embryonic lethality and radiation hypersensitivity mediated by Rad51 in mice lacking Brca2. *Nature*, *386*(6627), 804–810. https://doi.org/10.1038/386804a0

U.S. National Library of Medicine. SNP - NCBI. National Center for Biotechnology Information. https://www.ncbi.nlm.nih.gov/snp/?term=rs768349010

Venkitaraman, A. R. (2002). Cancer Susceptibility and the Functions of BRCA1 and BRCA2. *Cell*, *108*(2), 171–182. https://doi.org/10.1016/s0092-8674(02)00615-3

Wallace, D. C., Fan, W., & Procaccio, V. (2010). Mitochondrial energetics and therapeutics. *Annual review of pathology*, *5*, 297–348. https://doi.org/10.1146/annurev.pathol.4.110807.092314

Wang, Y., Zhang, L., Chen, Y., Li, M., Ha, M., & Li, S. (2020). Screening and identification of biomarkers associated with the diagnosis and prognosis of lung adenocarcinoma. *Journal of Clinical Laboratory Analysis*, *34*(10). https://doi.org/10.1002/jcla.23450

Wu, X., Ivanchenko, M. V., Al Jandal, H., Cicconet, M., Indzhykulian, A. A., & Corey, D. P. (2019). PKHD1L1 is a coat protein of hair-cell stereocilia and is required for normal hearing. *Nature Communications*, *10*(1). https://doi.org/10.1038/s41467-019-11712-w

Zheng, C., Quan, R., Xia, E. J., Bhandari, A., & Zhang, X. (2019). Original tumour suppressor gene polycystic kidney and hepatic disease 1-like 1 is associated with thyroid cancer cell progression. *Oncology letters*, *18*(3), 3227–3235. https://doi.org/10.3892/ol.2019.10632